Ichthyology & Herpetology 113, No. 1, 2025, 104–116

Illuminating the Early Life of Salamanders: Exploring Biofluorescence During Development

Jennifer Y. Lamb[1], Holden Cooper[2], Alexander Seymour[1], Matthew P. Davis[1], and Lynne Beaty[2]

Biofluorescence in tetrapods has rapidly become a captivating area of study. This phenomenon was previously identified to be widespread across amphibian diversity, but few studies have investigated biofluorescence in early life history stages. The aquatic environments inhabited by the early developmental stages of biphasic amphibians are different from those of terrestrial, post-metamorphic individuals. This could translate to differences in the presence and function of biofluorescence. In our study, we explored the biofluorescence of developing embryos and larvae of three species of mole salamander (*Ambystoma*) and one species of newt (*Notophthalmus*) in response to different excitation wavelengths. We discovered that the colors, intensity, and locations of maximal fluorescence varied ontogenically and by species. Although fluorescence occurred in response to both blue and green light, it was more prevalent and intense under blue excitation. Under blue excitation, we observed predominantly green fluorescence, but orange-red wavelengths were emitted in some taxa and developmental stages. We discuss intrinsic and external mechanisms that may be contributing to fluorescence in the eggs, embryos, and larvae of salamanders. We also use previously published criteria to generate hypotheses about the potential ecological significance of fluorescence in the aquatic life history stages of salamanders.

BIOFLUORESCENCE is a natural phenomenon in which high energy light absorbed by an organism is emitted into the environment at lower energy wavelengths. Numerous branches of the animal tree of life are biofluorescent. In the last ten years (2014–2024), there have been at least 81 publications documenting fluorescence in amphibians, reptiles, and mammals (Supplemental Appendix A; see Data Accessibility). These accounts include 43 distinct orders and 159 families of tetrapods. About half ($n = 42$) of those publications detail fluorescence in reptiles (including Aves), whereas 21 and 27 describe fluorescence in mammals and amphibians, respectively (Supplemental Appendix A; see Data Accessibility).

Biofluorescence is widespread among distantly related lineages of amphibians (Lamb and Davis, 2020). Twenty-two families of anurans, eight families of caudates, and two families of gymnophionans biofluoresce (Supplemental Appendix A; see Data Accessibility). Most recorded observations of biofluorescence in amphibians are for metamorphosed individuals. There are many fewer accounts of the presence or absence of biofluorescence during the embryonic and larval stages of amphibians (but see Lamb and Davis [2020] and Kong et al. [2023]). Lamb and Davis (2020) included the larvae of six species in two families of anurans (i.e., Hylidae, Ranidae) and three families of caudates (i.e., Ambystomatidae, Plethodontidae, Proteidae) in their broader survey. They confirmed the presence of biofluorescence in larval life history stages but did not document whether fluorescing patterns or colors changed with ontogeny or with different excitation wavelengths. Moreover, they did not observe biofluorescence in eggs and embryos of these species.

The potential mechanisms behind and biological functions of biofluorescence in amphibians are presently unknown for the majority of taxa (Marshall and Johnsen, 2017; Lamb and Davis, 2020; but see Taboada et al., 2017; Whitcher et al., 2024a, 2024b). For some amphibians, fluorescence in certain areas of the body is attributed to bony elements, secreted compounds, and pigments (Taboada et al., 2017; Goutte et al., 2019; Lamb and Davis, 2020; Whitcher et al., 2024b). Many potential sources of biofluorescence change throughout development in amphibians, and it is feasible that the functions of biofluorescence may also change with ontogeny. For example, fluorescence in amphibians is hypothesized to increase visibility of conspecifics (Taboada et al., 2017) and to contribute to communication (Whitcher et al., 2024b). However, for aquatic larvae, mates do not matter and mortality risk is high, so it may be more advantageous to be camouflaged. This variation in the landscape of selection could result in different patterns of biofluorescence. An ontogenetic perspective may help identify the mechanism(s) and potential functions of biofluorescence in amphibians.

Our objectives were to describe and compare patterns of biofluorescence across species of salamanders for which we could obtain an ontogenetic series and which were previously documented to be biofluorescent (Lamb and Davis, 2020). We focused on three species in Ambystomatidae, the Blue-spotted Salamander (*Ambystoma laterale*), Eastern Tiger Salamander (*A. tigrinum*), and Spotted Salamander (*A. maculatum*), and one species in Salamandridae, the Eastern Red-spotted Newt (*Notophthalmus viridescens viridescens*). We documented and quantified biofluorescent emissions in response to blue (440–460 nm) and green excitation (510–540 nm), with observations of fluorescent patterns in

[1] Department of Biology and Chemistry, St. Cloud State University, 720 4th Avenue South, St. Cloud, Minnesota 56301; ORCID: (JYL) 0000-0002-2677-1490; and (MPD) 0000-0001-5349-417X; Email: (JYL) jylamb@stcloudstate.edu; (AS) alex012494@gmail.com; and (MPD) mpdavis@stcloudstate.edu. Send correspondence to JYL.

[2] School of Science, Penn State Erie–The Behrend College, 4205 College Dr., Erie, Pennsylvania 16511; ORCID: (HC) 0009-0006-3331-8498; and (LB) 0000-0003-0778-1922; Email: (HC) hhc5057@psu.edu; and (LB) lzb345@psu.edu.

Submitted: 29 August 2024. Accepted: 14 January 2025. Associate Editor: T. Grande.

 DOI: 10.1643/h2024080 Published online: 6 March 2025

gross anatomy. Blue and green excitation wavelengths were chosen because they penetrate further in freshwater environments than do ultraviolet (UV) or violet light (Crump et al., 1999), and because they excite fluorescence in amphibians (Lamb and Davis, 2020; Supplemental Appendix A; see Data Accessibility).

MATERIALS AND METHODS

Fieldwork.—Populations of *Ambystoma laterale* and *A. tigrinum* were opportunistically sampled in central and south Minnesota from April through July in 2019, 2022, and 2023. We collected *A. laterale* from two small, ephemeral, fishless wetlands at Lake Maria State Park in Wright County. These wetlands occurred in primarily hardwood forests composed of maple (*Acer* spp.) and ash (*Fraxinus* spp.). Eggs were laid singly in submerged leaf litter or attached to graminoids in shallow (<60 cm) water. We revisited these ponds multiple times to capture larvae by using dip nets and soft-sided, collapsible, flat-bottomed minnow traps (Promar). We collected individuals of *A. tigrinum* from Crow-Hassan Reserve Park in Hennepin County and from Lake Maria State Park. Eggs and larvae were collected from two depressional prairie wetlands at Crow-Hassan Reserve Park. A large larval *A. tigrinum* was collected from an isolated wetland at Lake Maria State Park. The eggs of *Ambystoma tigrinum* were found in large masses attached to submerged graminoids. Multiple individuals were collected from several egg masses. Larval *A. tigrinum* were sampled using the same methods as described for *A. laterale*. All eggs and larvae of *A. laterale* and *A. tigrinum* were transported to St. Cloud State University for data collection. Eggs and embryos were maintained in a room with windows for access to natural light and in plastic containers with water from the original wetlands until hatching. This was done so that early larval stages could be observed. Data were collected from *A. laterale* and *A. tigrinum* while individuals were live or within ten to twenty minutes of euthanasia via a 20% solution of Benzocaine (Oragel; Altig, 1980; Lamb and Davis, 2020). All individuals of *A. laterale* and *A. tigrinum* were fixed in a 10% solution of buffered formalin and incorporated into SCSU's Herpetology Teaching Collection.

Ambystoma maculatum and *N. viridescens viridescens* were opportunistically collected on Penn State Behrend's campus in Erie County, Pennsylvania. The campus includes Great Lakes beech (*Fagus* spp.) and sugar maple (*Acer saccharum*) forests. Aquatic habitats include streams draining into Lake Erie, and ponds with variable hydroperiods. Egg surveys took place multiple times from May through June 2023. We sampled opaque and clear egg masses of *A. maculatum* and individuals at different stages of development. The eggs of *N. viridescens viridescens* were found by hand searching through aquatic vegetation for the singly laid eggs. We collected larval *A. maculatum* and *N. viridescens viridescens* from the same ponds. Larvae were captured in D-frame nets between May and August 2021 and again in August 2023. Salamander eggs and larvae were brought to laboratory facilities on Penn State Behrend's campus and photographed. Eggs and larvae were then returned to their respective ponds. We sampled metamorphosing and juvenile *A. maculatum* and *N. viridescens viridescens* in August 2021, August through October 2022, and August 2023. These individuals were encountered via visual and natural cover object surveys. Data collection from these individuals occurred either in the field or in the laboratory. All were released at their site of capture. It is possible that the same individual(s) were repeatedly examined for fluorescence because we revisited sites where previously sampled individuals were released.

Digital photography of biofluorescence.—We used digital photography to document fluorescing structures and to identify each individual's developmental stage (Shi and Boucaut, 1995). Images were either collected in the laboratory or the field. Images taken in a lab setting were collected under white light and then while under blue (440–460 nm) or green (510–540 nm) excitation lights and in a darkened room. If images were collected in the field, a blackout tent provided the necessary dark space for photography. All excitation lights were sourced from NIGHTSEA (blue: DFP RB-GR flashlight, Xite RB flashlights, or RB gooseneck lamps; green: DFP RB-GR flashlight, Xite GR flashlights, or GR gooseneck lamps). Images of fluorescence were captured through long pass filters (500 nm for blue excitation and 600 nm for green excitation lights) by a variety of different cameras (Canon EOS Rebel T7i DSLR camera with a 60 mm macro lens, Canon EOS Rebel T7 DSLR camera with a 18-55 mm lens, Olympus TG-5 digital camera, or with an iPhone XR).

Our goal was to document the fluorescence we observed, rather than to rigorously quantify how emission intensity varied between species or life stages. For this reason, some aspects of the photography environment and/or camera settings varied. For example, a glass petri dish was placed over the egg masses of *A. maculatum* to allow for clearer photos of embryos. Additionally, embryos within eggs, and small-bodied larvae, generally required longer exposure times (e.g., 4 seconds for images of embryos of *A. tigrinum*). The single egg of *N. viridescens viridescens* was imaged under a stereoscope (Wild Heerbrugg MDG 17) due to its small size. This individual was photographed daily under diffuse white and blue excitation lights. An iPhone XR camera was used to collect images through an eye piece and a long pass filter was placed over the objective lens.

Quantifying biofluorescent spectra.—Spectral data were collected from each species, and from most life stages, via two different Ocean Optics spectrometers. Fluorescent spectra were collected from *A. laterale* and from *A. tigrinum* with a FLAME-S-VIS-NIR-ES spectrometer connected to a 600 um UV/VIS fiber optic probe with a UV/VIS 200-2000 nm collimating lens. Dark calibration was used prior to data collection with this spectrometer (Lamb and Davis, 2020). Fluorescent spectra for *A. maculatum* and *N. viridescens viridescens* were collected with a USB2000+ spectrometer with a QR400-7-SR fiber optic probe calibrated with an Ocean Optics HG-2 mercury-argon wavelength calibration source. The same excitation light sources and long pass filters used during digital photography were also used when collecting spectral data. As in Lamb and Davis (2020), the long pass filter was placed between the probe and the specimen so that only fluorescent spectra would be recorded. For each species and life stage, four or five independent readings were collected from various regions of the body or egg mass. It was not always possible to position light sources and spectrometer probes at consistent distances from specimens. Specimens

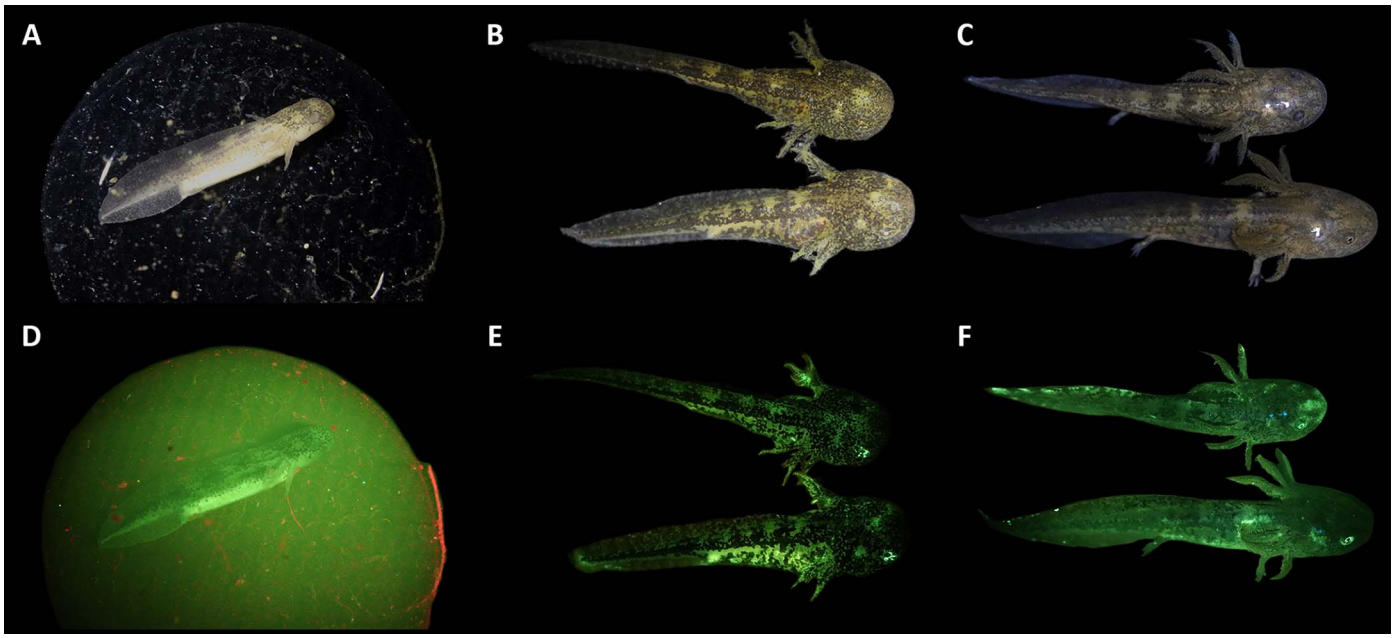

Fig. 1. Biofluorescence in the eggs and larvae of Eastern Tiger Salamanders (*Ambystoma tigrinum*) in response to blue excitation light. Areas of embryos (A), early-stage larvae (B), and late-stage larvae (C) with lighter pigments fluoresce green (D–F). Ventral surfaces fluoresce more brightly than do dorsal surfaces (D, E). There is minimal red fluorescence on the surface of the egg, but the jelly layers themselves fluoresce green (D).

differed in their overall size, and some species were measured within 20 minutes of euthanasia (i.e., *A. tigrinum*, *A. laterale*) whereas others were measured when live and capable of movement (i.e., *A. maculatum*, *N. viridescens viridescens*).

Analyzing emission spectra.—Spectral data collected by different spectrometers were analyzed separately but with the same approach. Spectra were averaged, smoothed, and summarized in the R package pavo (Maia et al., 2019). An average spectrum was found for each individual larva. Average spectral curves were calculated for each egg mass, or for an individual egg in the case of *N. viridescens viridescens*. We used the plotsmooth() function in pavo to identify the lowest span value for smoothing curves (span = 0.2). From these curves for each species and stage, we identified the wavelength at which fluorescent emission was the most intense, also known as the peak wavelength hue (H1; Montgomerie, 2006; Maia et al., 2019). If emission spectra contained more than one peak, we calculated the peak wavelength hue for each peak. Spectral curves were plotted using plot() in pavo.

RESULTS

Eggs and embryos

Ambystoma.—The egg jelly surrounding embryos of both *A. laterale* and *A. tigrinum* fluoresced in response to blue excitation light. Green fluorescent emissions were visible when eggs were submerged or held outside of water. Red fluorescence was also visible in a thin layer along the outer edges of the jelly, or scattered across it, for all individuals (Figs. 1, 2). Six embryos of *A. laterale* were collected around stage 5–7 (Shi and Boucaut, 1995). At this early stage of development, the darkly pigmented embryos did not appear to fluoresce. Three of these embryos continued to develop in the lab and were later observed at stages 22–27 (Shi and Boucaut, 1995). At this point, the egg jelly fluoresced green, but the darkly pigmented embryos within did not fluoresce (Supplemental Fig. 1; see Data Accessibility). Five embryos of *A. tigrinum* were collected from the field at developmental stages 31–34 (Shi and Boucaut, 1995). These individuals were close to hatching had already developed blotches of dark and light-yellow pigment across the dorsal and lateral surfaces of the body (Fig. 1A). Areas of yellow pigment on these surfaces appeared to fluoresce and were of a similar color and intensity as the surrounding egg jelly. The ventral surfaces of the developing embryos of *A. tigrinum* fluoresced brightly green and could clearly be differentiated from the surrounding egg jelly (Fig. 1D).

Eggs and embryos of *Ambystoma maculatum* from five egg masses also fluoresced in response to blue light (Supplemental Fig. 2; see Data Accessibility). Biofluorescent emissions could be seen when masses were submerged and when held outside of the water. The egg masses and egg capsules of *A. maculatum* fluoresced red, and the developing salamanders fluoresced green across stages 0–25 (Shi and Boucaut, 1995). The ventral surfaces of later-stage embryos of *A. maculatum* (stages 26–32; Shi and Boucaut, 1995) fluoresced bright green (Supplemental Fig. 2B; see Data Accessibility). In both early- ($n = 2$) and late-stage egg masses ($n = 2$), the green biofluorescence of the salamanders was largely obscured by the red biofluorescence of the egg capsules (Supplemental Fig. 2A; see Data Accessibility). We were able to collect fluorescence spectra for the eggs and embryos of two species (Fig. 3), including *A. maculatum*. The primary peak fluorescence measured from a single egg mass of *A. maculatum* (H1) was 685 nm, which falls within the red spectrum of visible light (Fig. 3B; Supplemental Table 1; see Data Accessibility).

Notophthalmus.—The single embryo of *N. viridescens viridescens* observed fluoresced in response to blue light (Fig. 4). The embryo and capsule both fluoresced green, although fluorescence was weaker for the egg capsule. The most intense

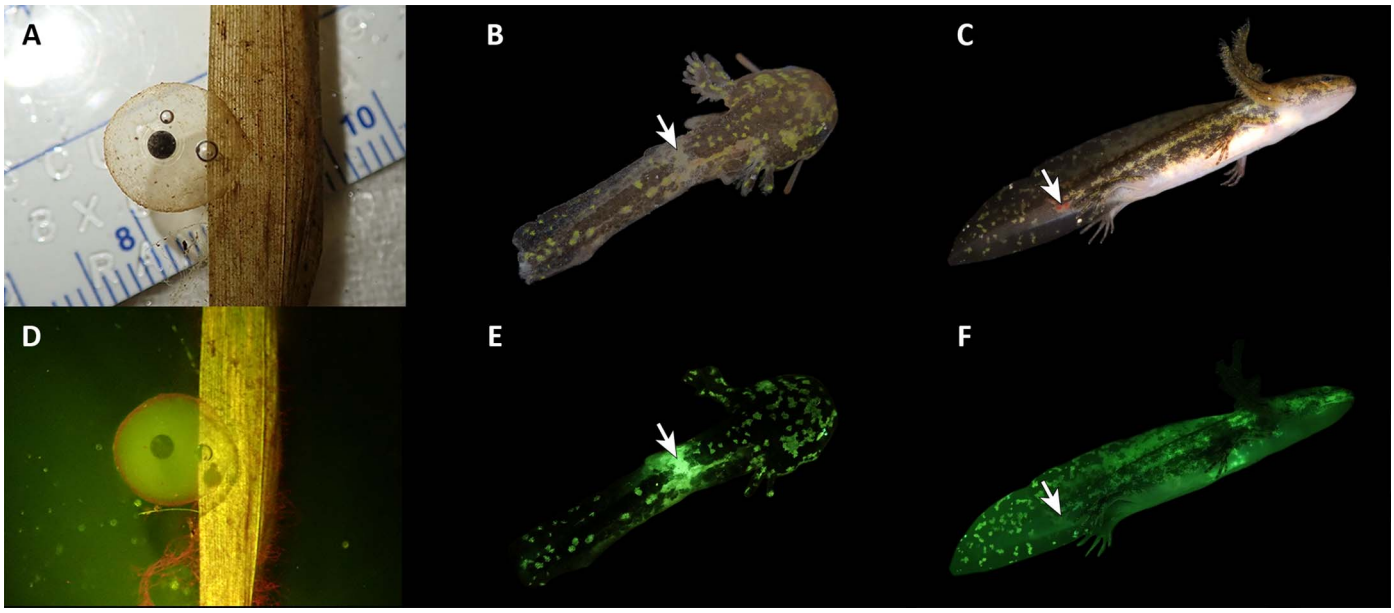

Fig. 2. Biofluorescence in the eggs and larvae of Blue-spotted Salamanders (*Ambystoma laterale*) in response to blue excitation light. The eggs (A), early-stage larvae (B), and late-stage larvae (C) fluoresce primarily green wavelengths of light (D–F). Red fluorescence is visible on the outer surface of the egg and is similar to fluorescence from epiphytes on the vegetation to which the egg is attached (D). Damaged tissues fluoresce intensely in the early-stage larvae (white arrows, B and E), but a small point of damage with visible blood in the late-stage larva is not comparably bright (white arrows, C and F).

fluorescence, or primary peak wavelength (H1), observed was 683 nm, and there was a secondary fluorescence peak at 550 nm (Fig. 3D; Supplemental Table 1; see Data Accessibility). Later in development (stages 26–32; Shi and Boucaut, 1995), the embryo of *N. viridescens viridescens* had brighter green markings on the ventral surface compared to the dorsal surface. Black pigment on the embryo contrasted against the green fluorescence (Fig. 4C, D).

Larvae

Ambystoma.—Fluorescence in response to blue excitation light occurred in hatchlings (around stage 34 for both species), early-stage larvae (34–39), and late-stage larvae (40 and beyond; Shi and Boucaut, 1995) for both *A. laterale* and *A. tigrinum*. We observed fluorescence in a total of 22 larval *A. laterale* and 28 larval *A. tigrinum*. The average wavelength of peak fluorescence (H1) was 533 ± 0 nm for *A. laterale* (measured from two late-stage larvae; snout-to-vent length = 16.5 ± 3.54 mm). This peak occurred at 535.5 ± 0.71 nm for the two individuals of *A. tigrinum* for which measurements were collected (late-stage larvae; snout-to-vent length = 72 ± 4.24 mm; Fig. 3; Supplemental Table 1; see Data Accessibility). These fluorescent emissions fall within the green spectrum of light. The relative intensity of fluorescence measured with the FLAME spectrometer was higher for the large larval *A. tigrinum* compared to the larval *A. laterale* (Fig. 3).

The relative intensity of fluorescence in response to blue light varied with the area of the body being viewed and by species. In both *A. laterale* and *A. tigrinum*, areas where larvae contained yellow and reflective white pigments in the skin or on the tailfin fluoresced brightly (Figs. 1, 2; Shi and Boucaut, 1995). Translucent areas of the tailfin also fluoresced both in and out of the water, although not as brightly as patterned areas of the body (Figs. 1, 2). The gastrointestinal tracts of small, early-stage larvae of *A. laterale* and *A. tigrinum*, which appear whitish yellow in daylight, fluoresced brightly green. In contrast, we observed that the ventral surfaces of late-stage larvae of *A. laterale* did not fluoresce brightly, whereas those of *A. tigrinum* did (Fig. 5). Fluorescence on the ventral surfaces of *A. laterale* was scattered and irregular. Occasionally, brighter reddish-pink or green fluorescing items within the gastrointestinal tract of some larger, late-stage larvae were observed (Fig. 5E). Some of the bones of the lower and upper jaws could be seen fluorescing through the skin in each species. The eyes, including lighter pigments in the iris but also areas behind the surface of the eye, fluoresced brightly throughout larval development (Figs. 1, 2, 5).

The condition of the specimens being observed impacted fluorescent emissions in response to blue excitation light. When larvae of *A. laterale* and *A. tigrinum* were accidentally damaged while they were positioned for photographs, the point of injury fluoresced green (Fig. 2B, E). However, blood vessels, and any points where blood was visible at the surface of the skin due to injury, did not fluoresce (Fig. 2C, F). To informally examine the effect of freezing on biofluorescence, we euthanized and then froze five larvae of *A. tigrinum* in 2 mL screw cap tubes at –20°C. We thawed and examined these individuals one week later. They had lost almost all darker pigments, and green fluorescence was apparent across the body more so than in larvae of a similar size and developmental stage that had not been frozen.

Larval *A. tigrinum* fluoresced red in response to green light, although at a much lower intensity compared to fluorescence in response to blue light (Fig. 6). These intensity measurements should not be statistically or quantitatively compared, but they do correspond with what we perceived when observing these specimens. Fluorescence in response to green excitation light was recorded for two individuals (late-stage larvae; snout-to-vent length = 72 ± 4.24 mm).

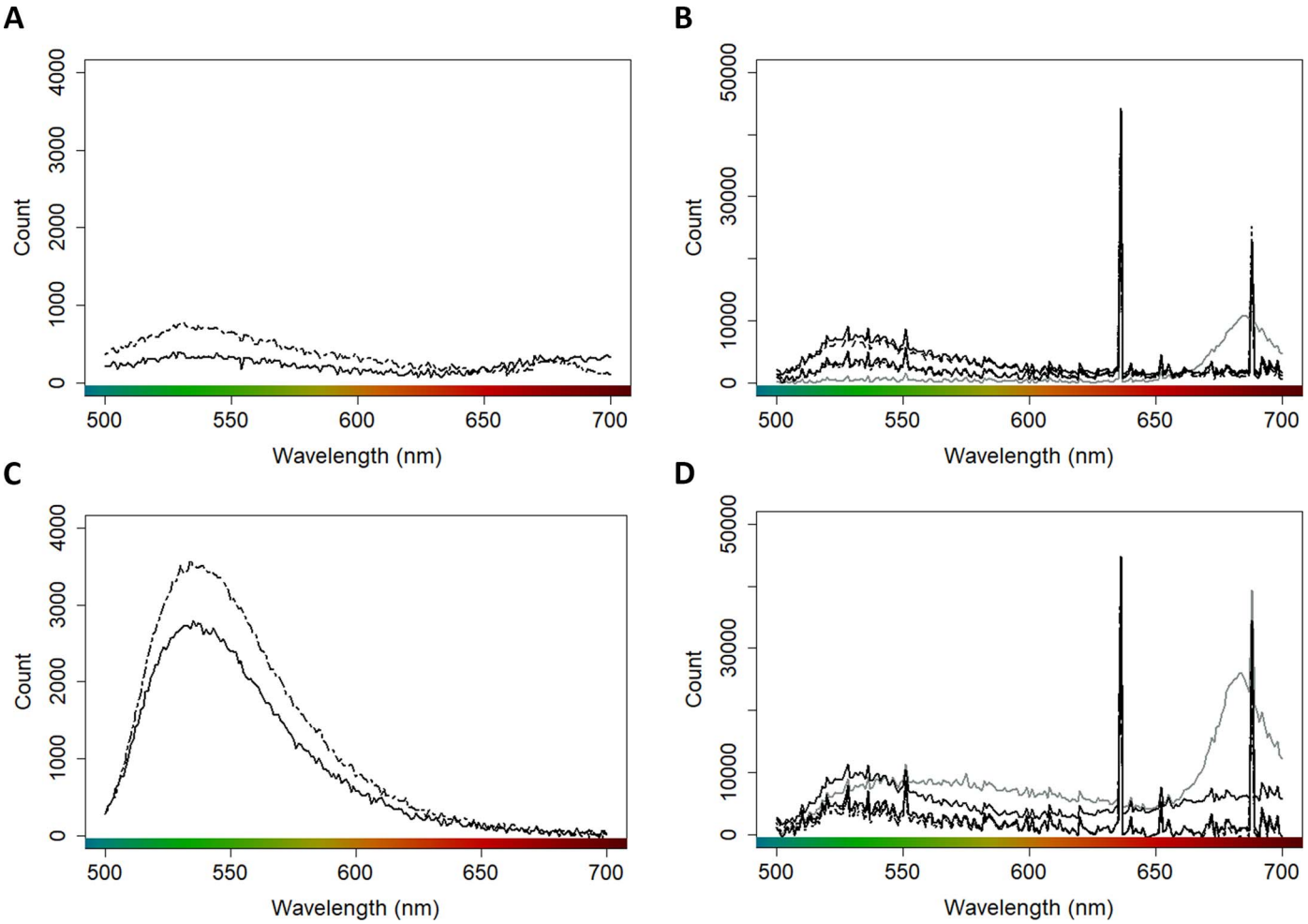

Fig. 3. Biofluorescence emission spectra in response to blue excitation light in the eggs, embryos, and larvae of salamanders. The data presented here represent averages for each egg or egg mass (gray lines), or individual larva (black lines), and are presented in their raw form (not smoothed). The y-axis represents sensor count data. The larvae of *Ambystoma laterale* ($n = 2$; A), *A. maculatum* ($n = 5$; B), *A. tigrinum* ($n = 1$; C), and *Notophthalmus viridescens viridescens* ($n = 5$; D) exhibit primary fluorescent emission peaks in the spectrum of green light (500–550 nm). Some larvae of *A. laterale* (A) and *N. viridescens viridescens* (D) also have secondary, smaller peaks or elevated readings in the spectrum of red light (625–700 nm). Primary fluorescent emission peaks for the eggs and embryos of *A. maculatum* (B) and *N. viridescens viridescens* (D) are in the spectrum of red light (625–700 nm). However, the single egg of the *N. viridescens viridescens* (D) that was measured also fluoresces in the spectrum of green light. The sharp spikes in B and D represent equipment measurement errors at approximately 636.5 and 689 nm, respectively. These spikes were excluded from spectral shape calculations in Supplemental Table 1 (see Data Accessibility).

The average wavelength of peak fluorescence (H1) was 606 ± 0 nm. These fluorescent emissions fall within the spectrum of red visible light (Fig. 6A). The average relative intensity of this red fluorescence was lower compared to the green fluorescence produced in response to blue excitation light (Figs. 3, 6; Supplemental Table 1; see Data Accessibility). However, similar patterns with respect to the gross anatomy fluorescing were apparent. The ventral surface fluoresced more strongly than did the dorsal surface, and areas with lighter pigments fluoresced brightly compared to areas with melanin (Fig. 5).

All of the larvae of *A. maculatum* observed fluoresced in response to blue light, but this species had limited fluorescence in response to green light. Fluorescence measurements were collected from five larvae. The peak fluorescence wavelength (H1) under blue light for these individuals was 532 ± 1 nm, appearing green in the visible spectrum (Fig. 3; Supplemental Table 1; see Data Accessibility). Patterns of biofluorescence exhibited significant changes throughout development for this species. Early larval *A. maculatum* (stages 35–39; Shi and Boucaut, 1995) fluoresced with the greatest intensity across their gill filaments, but their eyes and regions of the body lacking darker pigments also fluoresced (Fig. 7). In later-stage larva (stages 40–50; Shi and Boucaut, 1995), the ventral surfaces and iridophores had the most vibrant fluorescence, whereas fluorescence elsewhere, including the gill filaments, was reduced. Some of the bones of the lower and upper jaws, limbs, and digits could be seen fluorescing through the skin. The dorsal surfaces of later-stage larval *A. maculatum* weakly fluoresced green, but regions where yellow spots had begun to form had noticeably higher intensity (Fig. 7). Occasionally, pinkish-red fluorescence could be seen on the ventral midline some individuals. In general, specimens of *A. maculatum* did not display noticeable fluorescence under green excitation light (Supplemental Fig. 3; see Data Accessibility), and emission spectra were not recorded from larvae of this species for this light source.

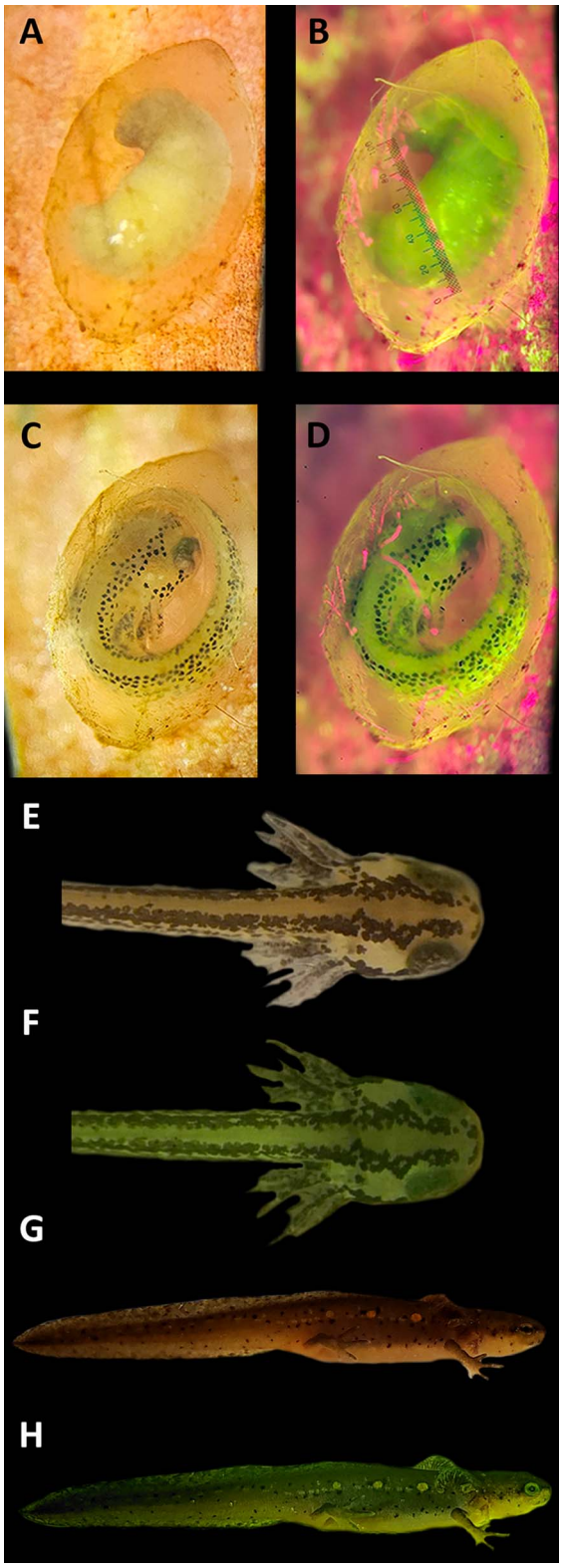

Fig. 4. Biofluorescence in the eggs and larvae of Eastern Red-spotted Newts (*Notophthalmus viridescens viridescens*) in response to blue excitation light. The eggs and embryos (A, C), early-stage larvae (E), and late-stage larvae (G) of *N. viridescens viridescens* fluoresce green in response to blue excitation light. Both early- and late-stage embryos (B, D) brightly fluoresce green. Early-stage larvae (F) are more vibrantly fluorescent than are those found in later stages of development (H). The dorsal red-orange spots seen in late-stage larvae, as well as some of the ventral surfaces of late-stage larvae appear to fluoresce orange wavelengths (H).

Notophthalmus.—Larvae of *N. viridescens viridescens* fluoresced in response to blue light and had limited fluorescence in response to green light. We measured fluorescence spectra in five larvae of this species. Peak fluorescence (H1) occurred in the green spectrum at 528 ± 2 nm, with two individuals having a secondary peak in the red spectrum at 692 ± 4 nm (Fig. 3; Supplemental Table 1; see Data Accessibility). The structures fluorescing, and the intensity of that fluorescence, changed throughout development. The single hatchling observed was still absorbing its yolk and displayed the most vibrant biofluorescence on its ventral surface where the yolk was visible under white light. In early-stage larvae (35–39; Shi and Boucaut, 1995), the entire body fluoresced bright green, and the developing dorsal orange-red spots, characteristic of this species' common name, fluoresced most intensely. These spots appeared white under white light. In later-stage larvae (40–50; Shi and Boucaut, 1995), dorsal fluorescence was less intense, with the exception of fluorescence from dorsal spots that were orange or red under white light. These spots fluoresced bright green and were distinct against the less-fluorescent dorsal surface of the body (Fig. 3). Gill rachis fluoresced more intensely than did filaments, and they appeared to retain the same level of brightness throughout development. Developing bones in the jaws and limbs fluoresced and were visible through the soft tissues. When exposed to green excitation light, larvae of *N. viridescens viridescens* displayed minimal biofluorescence (Supplemental Fig. 3; see Data Accessibility). They exhibited whole body red fluorescence with the exception of more darkly pigmented parts of the eye and the darkly pigmented line connecting the eye to the tip of the snout. Emission spectra were not recorded in response to green light for this species.

Metamorphs

Notophthalmus.—All efts exhibited both green and red fluorescence in response to blue excitation light (Fig. 8). Green fluorescence was present on both the dorsal and ventral surfaces. Fluorescent spectra collected from five individuals had an average, primary peak wavelength (H1) equaling 526 ± 0 nm and a smaller, secondary wavelength of 605.2 ± 0.45 nm (Fig. 8C). In some of the efts observed, the bright red dorsal spots fluoresced green, while in others they fluoresced an orange-red (Fig. 8B). Some of the individuals that had red-orange fluorescent dorsal spots in response to blue light also exhibited dark orange fluorescence on the majority of their tail (Fig. 8). When exposed to green excitation light, efts fluoresced red across all surfaces, and the red spots fluoresced more intensely than did other surfaces (Supplemental Fig. 3F; see Data Accessibility). Bones of the digits could be seen fluorescing through the skin under both blue and green excitation lights.

DISCUSSION

We suspect that multiple mechanisms are responsible for the fluorescence observed in salamander eggs. Photosynthetic symbionts could be producing red fluorescent wavelengths (Kerney et al., 2011). This fluorescence was prominent in the eggs of *A. maculatum* (Supplemental Fig. 2; see Data Accessibility), a species that is well known for symbiotic associations with algae (Kerney et al., 2011; Kim et al., 2014). We also document red fluorescence on the surfaces of eggs of

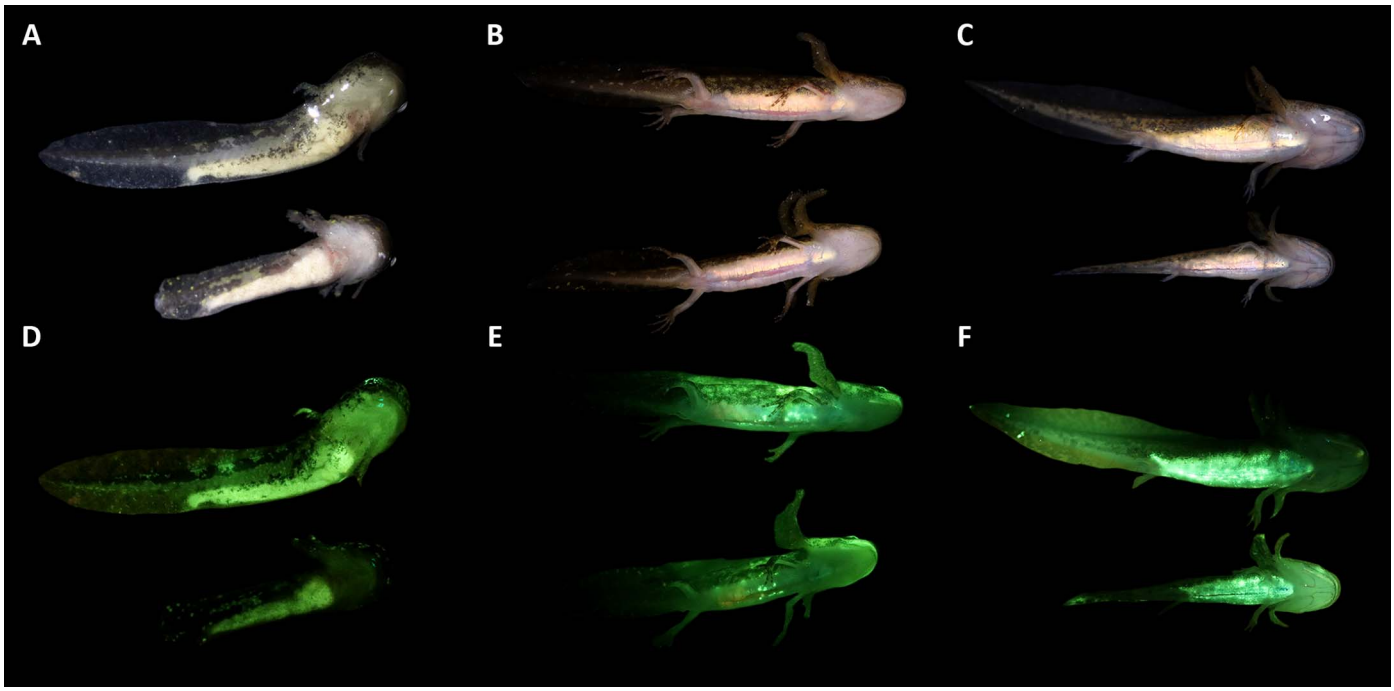

Fig. 5. Ventral biofluorescence in response to blue excitation light. Ventral fluorescence varies with species and ontogeny. Green fluorescence is brighter in larval *A. tigrinum* (A and D top, C, F) than it is in *A. laterale* (A and D bottom, B, E). Early- (A) and late-stage (B, C) larval *Ambystoma* have bright white or reflective ventral surfaces under white light. These surfaces emit bright green fluorescence (D–F), but are more fluorescent in late-stage *A. tigrinum* (F) than in late-stage *A. laterale* (E).

A. laterale, *A. tigrinum*, and *N. viridescens viridescens* (Figs. 1, 2, 4). Amphibian eggs can be colonized by different microbes, including algae and photosynthetic bacteria (Kim et al., 2014; Anslan et al., 2021). Photosynthetic organisms, including symbiotic algae, fluoresce red in response to blue excitation light (Kerney et al., 2011). The spectrometer measured red fluorescence in the egg of *N. viridescens viridescens* (Fig. 4; Supplemental Table 1; see Data Accessibility), but in images it appears this fluorescence may belong to the grammanoid to which the egg is attached (Fig. 4). The green fluorescence we document could be produced by compounds within amphibian eggs. To our knowledge, no studies have identified whether components of amphibian eggs, such as mucopolysaccharides and mucoproteins in the capsule layers (Duellman and Trueb, 1994), biofluoresce. Alternatively, the green fluorescence could be due to egg capsules absorbing components from the water column. Both the egg capsules and the perivitelline space absorb water after oviposition (Salthe, 1965), and water from our field sites fluoresced green.

Variation in the intensity of fluorescence in early embryos may be caused by differences in melanin concentration. The embryo of *N. viridescens viridescens* fluoresced green as early as developmental stage 23 (Shi and Boucaut, 1995; Fig. 3B), whereas embryos of *A. laterale* observed at a similar developmental stage did not (Fig. 2; Supplemental Fig. 1; see Data Accessibility). The eggs of *N. viridescens viridescens* are "light to dark brown," whereas those of *A. laterale* are "darkly pigmented" (Petranka, 1998). This difference in pigmentation may be due to the species utilizing different

Fig. 6. Eastern Tiger Salamander (*A. tigrinum*) larvae fluoresce red in response to green excitation light. Multiple independent spectral readings were averaged for two larvae and are presented here in their raw form (not smoothed; A). Individuals are represented with different line types. Black lines represent measurements from the ventral surface. The y-axis represents sensor count data. The primary emission peaks for both individuals and surfaces are in the spectrum of orange-red light. Areas with lighter or reflective pigments in white light (B) are responsible for the red fluorescence observed (C).

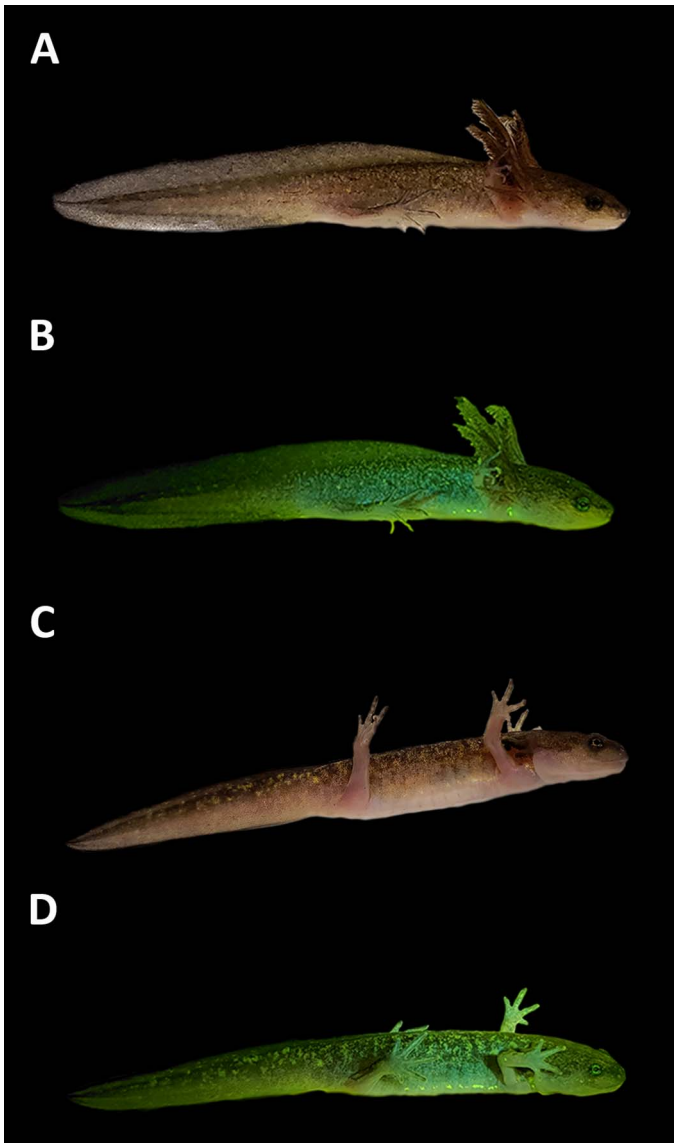

Fig. 7. Larval Spotted Salamanders (*A. maculatum*) biofluoresce green in response to blue excitation light. Early- (A) and late-stage (C) *A. maculatum* fluoresce green (B and D, respectively) in response to blue light. In both stages, fluorescence is brighter in areas that appear lighter under white light (A, C), including ventral surfaces. Areas with iridophores fluoresce especially brightly (B, D).

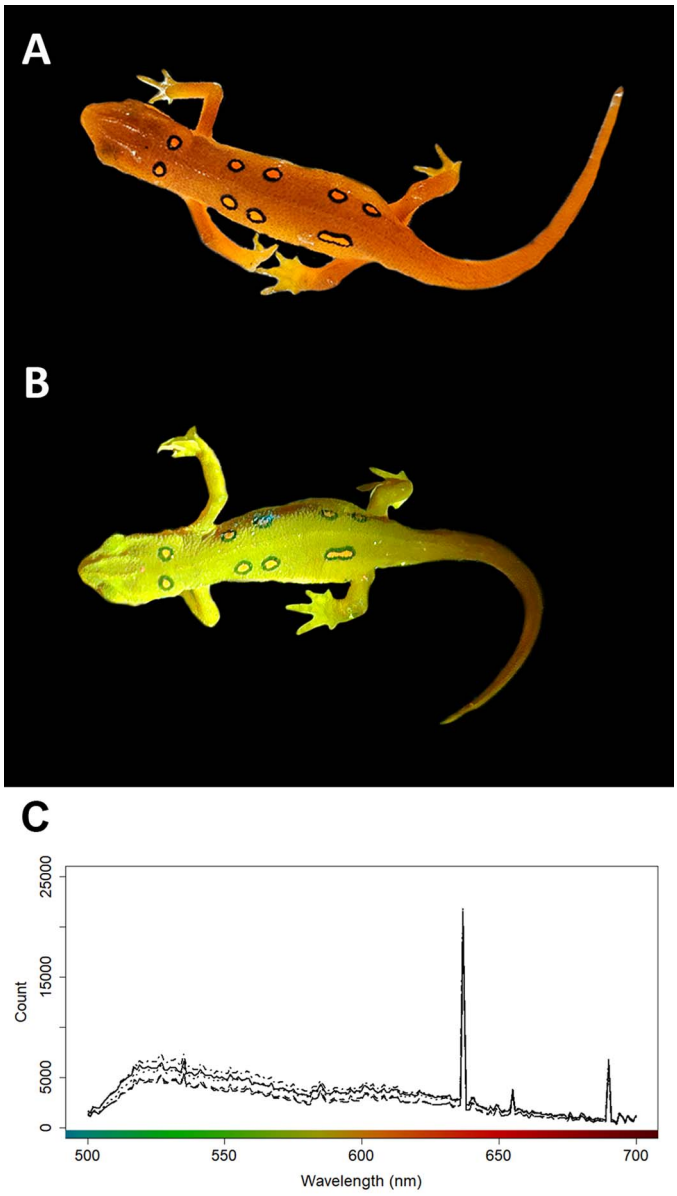

Fig. 8. Biofluorescence of Eastern Red-spotted Newt (*N. viridescens viridescens*) efts in response to blue excitation light. Post-metamorphic *N. viridescens viridescens* (i.e., efts; A) brightly fluoresce green in response to blue excitation light (B). In some individuals, the red-orange spots located on the dorsal surface of the eft (A) fluoresce green, while in others they fluoresce orange (B). The primary peak wavelength emitted is within the green spectrum, but there is a smaller, secondary peak within the red spectrum (C).

microhabitats for oviposition. *Notophthalmus viridescens viridescens* typically lay eggs singly and tuck them into aquatic vegetation (Petranka, 1998; Altig and McDiarmid, 2015) where they are likely shaded from damaging ultraviolet wavelengths. Amphibians that deposit their eggs in habitats with more ultraviolet exposure tend to have darkly pigmented embryos (Duellman and Trueb, 1994; Petranka, 1998; Altig and McDiarmid, 2015).

Our observations of fluorescence in larval amphibians in response to blue light expand on the findings of Lamb and Davis (2020). As in that study, we saw that fluorescence in larval salamanders primarily included green wavelengths (Fig. 3). Areas with yellow, red, and/or white pigments, and the ventral surfaces, fluoresced intensely (Figs. 1, 2, 4, 5, 7). We also saw bony fluorescence, particularly in the digits, limbs, and jaw. However, unlike Lamb and Davis (2020), we observed orange-red fluorescence in some amphibian larvae (Figs. 3–5). This fluorescence could be caused by multiple mechanisms. Larval newts form red dorsolateral spots as they develop (Fig. 4G). In efts, these spots fluoresce orange-red under blue light (Fig. 8). Orange-red fluorescence visible ventrally or laterally could also come from the gastrointestinal tract. Larval salamanders sometimes ingest plant or algal matter, and they actively feed on small arthropods, including crustaceans (Brophy, 1980). We lack information about fluorescence in freshwater crustaceans, but some marine crustaceans fluoresce red under blue excitation light (Juhasz-Dora et al., 2024). Alternatively, the intestines of

larval salamanders may inherently fluoresce. Autofluorescence in the yellow-green spectrum occurs in the intestinal tissues of larval clawed frogs (genus *Xenopus*; Yergeau et al., 2009). Careful dissection of larval amphibians to observe the source of fluorescence would be an interesting direction for future studies.

Different species of larval salamanders varied in the intensity of their fluorescence, and it appears that fluorescence in response to blue light is most prominent in *A. tigrinum*. Green fluorescence measured from this species appeared more intense than it was for *A. laterale* (Figs. 3, 5). This corresponds with observations made of fluorescence in metamorphosed individuals of the same taxa (Lamb and Davis, 2020). Interestingly, the ventral surfaces of *A. tigrinum* fluoresced brighter than those of other congeners (Fig. 5). The skin of larval amphibians is thin and often translucent, and the peritonea of other larval *Ambystoma* (i.e., axolotls, *A. mexicanum*) are densely populated with iridophores (Dalton and Hoerter, 1974). Iridophores contain components such as guanine which could be the mechanism behind the fluorescence observed (Marshall and Johnsen, 2017).

Biofluorescence varied among individuals within the same species, potentially due to variation in an individual's health or other factors. Pigments like carotenoids can be costly to produce and maintain (McGraw, 2006). Individuals that do not fluoresce brightly may not be able to afford those energetic costs. In the case of the efts of *N. viridescens viridescens*, variation in fluorescence could also correlate with toxicity. Efts that are older (Brodie, 1968) and efts with more red spots (Spicer et al., 2018) have higher levels of toxins in their skin compared to those with fewer red spots. These spots fluoresced brightly under both blue and green excitation (Fig. 8; Supplemental Fig. 3; see Data Accessibility). Whether fluorescence contributes to aposematism in the efts of *N. viridescens viridescens* warrants further investigation. There have been some creative studies which have utilized painted clay models to test the hypothesis that fluorescence contributes to aposematism in frogs (Whitcher et al., 2024a) and fireflies (Wilcox and Lewis, 2019). However, these studies have failed to support that hypothesis. Still, future studies should examine how an individual amphibian's body condition might influence fluorescence.

There are likely additional, non-pigment-based mechanisms behind biofluorescence in larval salamanders. Injured specimens fluoresced intensely at the point of damage (Fig. 2B, E), but visible blood at the surface of the tissue did not notably fluoresce (see Fig. 2C, F). Small larvae frozen at –20°C fluoresced uniformly across the body. This suggests that observations of fluorescence made from frozen tissues should be interpreted cautiously. Freezing ruptures cells and may degrade pigments, both of which likely alter the appearance of fluorescence. Taboada et al. (2017) identified hyloins in the lymph and dermal secretions of some anurans that were largely responsible for non-pigment-based fluorescence. Lamb and Davis (2020) also point to seemingly non-pigment-based fluorescence across amphibians that lack bold, colorful patterns. Identifying the mechanisms behind fluorescence across amphibian groups will likely require an interdisciplinary approach that combines observations like these with histological and biochemical approaches.

Exploring potential functions.—Marshall and Johnsen (2017) present a checklist that is helpful in considering whether observed biofluorescence might be ecologically relevant. Their criteria include that (1) fluorescence occurs on part(s) of the organism that are visible, (2) the wavelengths fluoresced are within the spectral sensitivities of potential viewers, (3) the wavelengths that excite fluorescence are prominent in the natural lighting conditions experienced by the organism, and (4) the fluorescent area(s) are visible during behaviors that could impact an individual's fitness. Whitcher et al. (2024b) applied Marshall and Johnsen's (2017) criteria to their survey for fluorescence, which focused on metamorphosed anurans. They concluded that just over half of the anurans tested, a total of 86 species, met these criteria. We suggest that biofluorescence in the species of larval salamanders we tested meets Criteria 1, 2, and 4 from Marshall and Johnsen (2017) and hypothesize that if biofluorescence is ecologically significant in this life history stage, then it contributes to camouflage.

Fluorescence in larval salamanders occurs on surfaces of the body that would be visible when the animals are at rest and when moving through the water column (Criterion 1). During the day, larval salamanders are often found on the bottoms of their aquatic habitats (Anderson and Graham, 1967; Hassinger et al., 1970; Branch and Altig, 1981). They may be buried and out of sight, but they do also rest on the surfaces of the substrate, detritus, and aquatic vegetation. In these instances, the dorsal and lateral sides of the body and tail might be visible. The bodies and tails of larval salamanders are typically covered by patches, spots, or stripes that fluoresce (Figs. 1, 2, 4, 7). However, the ventral surfaces of larvae tend to fluoresce more noticeably than do the dorsal or lateral surfaces. Ventral surfaces would be visible either from the side or below when the animals are foraging, swimming, or floating in the water column (Anderson and Graham, 1967; Hassinger et al., 1970; Branch and Altig, 1981). Fluorescent emissions in response to blue excitation were brighter than emissions in response to green excitation (Figs. 3, 6; Supplemental Table 1; see Data Accessibility). For this reason, we speculate that the wavelengths emitted when exposed to blue light are more relevant.

The green to red fluorescent emissions produced by larval salamanders (Fig. 3; Supplemental Table 1; see Data Accessibility) are within the spectral sensitivities of other amphibians (Criterion 2). Larval salamanders predate smaller amphibians and are depredated by congeners (Lannoo, 2005). Broadly speaking, the photoreceptor cells of larval amphibians can detect longer wavelengths of light (Fouilloux et al., 2022). For example, potential prey, like the tadpoles of Northern Leopard Frogs (*Lithobates pipiens*), are sensitive to both green (medium wavelength sensitive rods and cones $\lambda_{max} = 527$ nm) and red (long wavelength sensitive cones $\lambda_{max} = 620$ nm) wavelengths of light (Liebman and Entine, 1968). Larval *A. tigrinum* are sensitive to both green (medium wavelength sensitive rod $\lambda_{max} = 516$ nm), yellow (long wavelength sensitive cones $\lambda_{max} = 584$, 586 nm), and red wavelengths (Isayama et al., 2014).

Larval salamanders are also prey for many aquatic invertebrates that can perceive green to red wavelengths (Immonen et al., 2014; Futahashi et al., 2015; Guignard et al., 2022; Criterion 2). Potential predators of larval salamanders include dragonfly nymphs (order Odonata), diving beetles (order Coleoptera), as well as belostomatids and notonectids

(order Hemiptera; Lannoo, 2005; Stretz et al., 2019). Visual acuity (Feller et al., 2021) and color sensitivities vary across these groups, but several have photoreceptors or express opsins sensitive to medium and longer wavelengths of light (Immonen et al., 2014; Futahashi et al., 2015; Guignard et al., 2022). For example, odonate nymphs that predate larval salamanders (e.g., families Aeshnidae and Libellulidae; Lannoo, 2005) express multiple visual opsins that are sensitive to long wavelengths in the green spectrum (i.e., ca. $\lambda_{max} = 530$ nm; Futahashi et al., 2015; Guignard et al., 2022) and notonectids have photoreceptors with λ_{max} that fall within 500–600 nm (see Immonen et al., 2014: fig. 1a).

Shorter wavelengths, like UV and blue light, may not be available throughout freshwater aquatic habitats, or at all times of the year in these environments. In freshwater systems, UV and blue light attenuate at shallower depths in the water column than they do in marine systems. This is due to absorption and scattering by dissolved organic carbons and suspended particulates (Lean, 1998; Crump et al., 1999). Algae and aquatic plants can also contribute to light attenuation, scattering, and shading (Krause-Jensen and Sand-Jensen, 1998; Lean, 1998; Crump et al., 1999; Arts et al., 2000; Cronin et al., 2014; Hornbach et al., 2020). Due to their density, plants likely have a major impact on the light environment in a freshwater wetland during the height of the growing season. Because of these factors, there may be little illumination below about 50 cm in freshwater wetlands (Crump et al., 1999; Arts et al., 2000). The wetlands used for breeding by the mole salamanders and newts studied here are often shallow (i.e., $\leq$1.5 m), ephemeral to semi-permanent, with ample aquatic vegetation (Lannoo, 2005). Larval salamanders utilize multiple depths in these wetlands, including depths to which blue light may penetrate. However, additional data describing water turbidity, as well as irradiance and transmission spectra at varying depths in these environments, are needed. Without those data, we cannot evaluate Marshall and Johnsen's (2017) third criterion regarding the prevalence of excitation wavelengths where larval salamanders occur.

We hypothesize that if biofluorescence in larval salamanders is ecologically significant (Marshall and Johnsen, 2017), it most likely contributes to camouflage. Green fluorescence in free-swimming larvae could help individuals blend in with the green-fluorescing water column when moving through open areas (Criterion 4). Fluorescence of the lateral and dorsal sides of larvae corresponds with mottled areas of light pigments (Figs. 1, 2, 4, 7). These seemingly random patterns may obscure a larva's body shape and contribute to disruptive camouflage in the water column (Altig, 1972). Similarly, countershading, having a brighter ventral and darker dorsal surface, may be an important method of camouflage for this life stage (Altig, 1972; Thibaudeau and Altig, 2012). Larval salamanders will forage for prey, including smaller salamander larvae (Lannoo, 2005), by suspending themselves in the water column at various depths (Anderson and Graham, 1967; Hassinger et al., 1970; Branch and Altig, 1981). In these scenarios, fluorescence from the ventral surface may reduce an individual's shadow when viewed from below or contribute to background matching from different angles (Kelley et al., 2017; Kohler et al., 2019). At this point, we lack studies that explicitly test the role of biofluorescence in amphibian camouflage. However, camouflage via background matching and/or disruptive patterns appears to be a function of biofluorescence in some marine fishes (Sparks et al., 2014; Anthes et al., 2016).

For species that oviposit in exposed locations in wetlands (e.g., many species of *Ambystoma*), we hypothesize that fluorescence contributes to camouflage via background matching. Fluorescence may help eggs or egg masses color match vegetation and/or the background fluorescence from the water column. Egg masses of *A. maculatum* and *A. tigrinum* are attached to submerged vegetation or woody structures (Petranka, 1998; Lannoo, 2005). The eggs are exposed and visible (Criterion 1). Adults of these species do not defend their eggs, and embryos are vulnerable to predation from other salamanders (e.g., *Notophthalmus*; Lannoo, 2005), invertebrates (e.g., odonate nymphs; Ward and Sexton, 1981; Gunzburger and Travis, 2005), and, in some cases, from tadpoles (e.g., Wood Frogs [*Lithobates sylvaticus*]; Petranka et al., 1998; Criterion 4). Many of these potential predators can visualize the red and green wavelengths fluoresced by salamander eggs (Criterion 2). As previously stated, we need additional data regarding the light environments of these wetlands before concluding that Marshall and Johnsen's (2017) third criterion is met by this life history stage.

Caveats and future directions.—There are several important caveats to keep in mind regarding our results. Although we have included eggs, embryos, larvae, and efts, our sample sizes for some species, life stages, and data types (i.e., spectral data) are limited. Our spectral dataset is additionally restrictive because we cannot make statistical comparisons with respect to fluorescence intensity due to variation in the placement of light sources and probes. Light and probe geometry would not typically affect the emission wavelengths measured, but it does introduce noise into measurements of intensity or brightness. Importantly, this survey does not consider the impact of potential environmental factors on fluorescence in amphibian larvae. Our data suggest that some aspects of fluorescence correlate with the overall color and pattern of larval amphibians. However, these traits are influenced by geographic location as well as local environmental factors in many species during the larval period (Thibaudeau and Altig, 2012). For example, a larva's brightness or the colors they exhibit can vary with time of day (Altig, 1972), photoperiod (Rodríguez-Rodríguez et al., 2021), temperature (Garcia et al., 2003; Rodríguez-Rodríguez et al., 2021; Hird et al., 2023), background or substrate reflectance (Polo-Cavia and Gomez-Mestre, 2017; Rodríguez-Rodríguez et al., 2021; Liedtke et al., 2023), and, potentially, water clarity (Altig, 1972; Thibaudeau and Altig, 2012). Knowing this, future efforts to document and quantify fluorescence in larval amphibians should endeavor to account for or explicitly test the impact of these factors on both fluoresced and reflected color and pattern.

We suggest that researchers take advantage of any opportunity to test amphibian larvae for biofluorescence. Surveys that cast a wide taxonomic net are more likely to uncover unique variation or additional practical applications for the use of fluorescence (see Smith et al., 2018). There are surprising gaps in our knowledge of the biology and ecology of amphibian larvae, including for species in North America (Altig, 2018). Our review of pertinent literature shows that the number of studies documenting amphibian biofluorescence is growing rapidly

($n = 27$), but also that larval amphibians are being left behind (i.e., only Kong et al. [2023] and Lamb and Davis [2020] report testing fluorescence in larvae; Supplemental Appendix A; see Data Accessibility). If a targeted approach is preferred, we suggest that researchers use a combination of morphological and ecological traits to guide their surveys for biofluorescence in larval amphibians. We predict that larvae that exhibit bright colors, or those with translucent skin and white peritonea, are likely to fluoresce. Some of these same traits have been targeted by other authors studying fluorescence in metamorphosed anurans (e.g., Taboada et al., 2017). Additionally, larvae that are noxious or toxic, or that forage while exposed in shallow or clear waters, may exhibit interesting fluorescence. Finally, we suggest that species with prominent fluorescence as adults be examined as larvae. Adding to our understanding of fluorescence in the larval stage can help us better understand fluorescence in metamorphosed individuals.

Our study stands out in that it is one of the few that document and quantify biofluorescence across the aquatic life stages of amphibians (Supplemental Appendix A; see Data Accessibility). By revealing the presence of fluorescence in the eggs, developing embryos, and larvae of four salamander species that represent two families, we take important strides in bridging knowledge gaps identified by Lamb and Davis (2020). We delve into potential mechanisms of biofluorescence and highlight areas where further research is needed. These insights carve paths toward a deeper understanding of the ecological significance that biofluorescence might hold for amphibians across their life histories.

DATA ACCESSIBILITY

Supplemental material is available at https://www.ichthyologyandherpetology.org/h2024080. Unless an alternative copyright or statement noting that a figure is reprinted from a previous source is noted in a figure caption, the published images and illustrations in this article are licensed by the American Society of Ichthyologists and Herpetologists for use if the use includes a citation to the original source (American Society of Ichthyologists and Herpetologists, the DOI of the *Ichthyology & Herpetology* article, and any individual image credits listed in the figure caption) in accordance with the Creative Commons Attribution CC BY License.

AI STATEMENT

The authors declare that they used Artificial Intelligence (AI) to organize taxonomic information for a supplementary table (Supplemental Appendix A; see Data Accessibility). Specifically, we used ChatGPT to match species names for taxa from Newar et al. (2024) with the families to which they belonged. Family names identified by ChatGPT were then checked by JYL against other online databases for accuracy and used in Supplemental Appendix A.

ACKNOWLEDGMENTS

We would like to thank B. R. Richards, B. C. Morris, E. Parker, and S. Nutile for their help in the field, B. Reinke for her guidance regarding the analysis of spectral data, and B. Last for her assistance with equipment. Financial support included SCSU Early Career and SCSU Faculty Improvement Grants (JYL), SCSU Faculty Improvement and Midcareer Grant (MPD), SCSU Hellervik Award (MPD), a Minnesota Herpetological Society Grant (AMS and JYL), an SCSU Student-Mentor Collaboration Grant (AMS), two Penn State Behrend Research Office Undergraduate Research Grants (HHC), and resources from the Penn State Behrend School of Science (LEB). All field and laboratory work in Minnesota was completed according to SCSU IACUC protocols (17-112 and 17-130), MN Department of Natural Resource permits (Special Permit #24194 and #35353, PAT #201878 and #202334), and a Special Use Permit from the Three Rivers Park District. All work in Pennsylvania was done in accordance with PA Fish and Boat Commission (permit numbers: 2021-01-0086, 2022-01-0284, 2023-01-0095) and Penn State's IACUC (PROTO202101889). Institutional support was provided by St. Cloud State University in the use of facilities in Wick Science Building and the Integrated Science and Engineering Laboratory Facility (ISELF) and by Penn State Behrend in the Nick and Benson Buildings.

LITERATURE CITED

Altig, R. 1972. Notes on the larvae and premetamorphic tadpoles of four *Hyla* and three *Rana* with notes on tadpole color patterns. Journal of the Elisha Mitchell Scientific Society 88:113–119.

Altig, R. 1980. A convenient killing agent for amphibians. Herpetological Review 11:35.

Altig, R. 2018. Fifty-three years a tadpole. Journal of Herpetology 52:1–5.

Altig, R., and R. McDiarmid. 2015. Handbook of Larval Amphibians of the United States and Canada. Cornell University Press, Ithaca, New York.

Anderson, J. D., and R. E. Graham. 1967. Vertical migration and stratification of larval *Ambystoma*. Copeia 1967:371–374.

Anslan, S., M. Sachs, L. Rancilhac, H. Brinkmann, J. Petersen, S. Künzel, A. Schwarz, H. Arndt, R. Kerney, and M. Vences. 2021. Diversity and substrate-specificity of green algae and other micro-eukaryotes colonizing amphibian clutches in Germany, revealed by DNA metabarcoding. The Science of Nature 108:29.

Anthes, N., J. Theobald, T. Gerlach, M. G. Meadows, and N. K. Michiels. 2016. Diversity and ecological correlates of red fluorescence in marine fishes. Frontiers in Ecology and Evolution 4:126.

Arts, M. T., R. D. Robarts, F. Kasai, M. J. Waiser, V. P. Tumber, A. J. Plante, H. Rai, and H. J. de Lange. 2000. The attenuation of ultraviolet radiation in high dissolved organic carbon waters of wetlands and lakes on the northern Great Plains. Limnology and Oceanography 45:292–299.

Branch, L. C., and R. Altig. 1981. Nocturnal stratification of three species of *Ambystoma* larvae. Copeia 1981:870–873.

Brodie, E. D., Jr. 1968. Investigations on the skin toxin of the red-spotted newt, *Notophthalmus viridescens viridescens*. American Midland Naturalist 80:276–280.

Brophy, T. E. 1980. Food habits of sympatric larval *Ambystoma tigrinum* and *Notophthalmus viridescens*. Journal of Herpetology 14:1–6.

Cronin, T. W., S. Johnsen, N. J. Marshall, and E. J. Warrant. 2014. Visual Ecology. Princeton University Press, Princeton, New Jersey.

Crump, D., D. Lean, M. Berrill, D. Coulson, and L. Toy. 1999. Spectral irradiance in pond water: influence of water chemistry. Photochemistry and Photobiology 70:893–901.

Dalton, H. C., and J. D. Hoerter. 1974. Patterns of purine synthesis related to iridophore development in the wild type, melanoid, and axanthic strains of the Mexican axolotl, *Ambystoma mexicanum* (Shaw). Developmental Biology 36:245–251.

Duellman, W. E., and L. Trueb. 1994. Biology of Amphibians. Johns Hopkins University Press, Baltimore, Maryland.

Feller, K. D., C. R. Sharkey, A. McDuffee-Altekruse, H. D. Bracken-Grissom, N. P. Lord, M. L. Porter, and L. E. Schweikert. 2021. Surf and turf vision: patterns and predictors of visual acuity in compound eye evolution. Arthropod Structure & Development 60:101002.

Fouilloux, C. A., C. A. M. Yovanovich, and B. Rojas. 2022. Tadpole responses to environments with limited visibility: what we (don't) know and perspectives for a sharper future. Frontiers in Ecology and Evolution 9:766725.

Futahashi, R., R. Kawahara-Miki, M. Kinoshita, K. Yoshitake, S. Yajima, K. Arikawa, and T. Fukatsu. 2015. Extraordinary diversity of visual opsin genes in dragonflies. Proceedings of the National Academy of Sciences of the United States of America 112:E1247–E1256.

Garcia, T. S., R. Straus, and A. Sih. 2003. Temperature and ontogenetic effects on color change in the larval salamander species *Ambystoma barbouri* and *Ambystoma texanum*. Canadian Journal of Zoology 81:710–715.

Goutte, S., M. J. Mason, M. M. Antoniazzi, C. Jared, D. Merle, L. Cazes, L. F. Toledo, H. El-Hafci, S. Pallu, H. Portier, and S. Schramm. 2019. Intense bone fluorescence reveals hidden patterns in pumpkin toadlets. Scientific Reports 9:5388.

Guignard, Q., J. D. Allison, and B. Slippers. 2022. The evolution of insect visual opsin genes with specific consideration of the influence of ocelli and life history traits. BMC Ecology and Evolution 22:2.

Gunzburger, M. S., and J. Travis. 2005. Critical literature review of the evidence for unpalatability of amphibian eggs and larvae. Journal of Herpetology 39:547–571.

Hassinger, D. D., J. D. Anderson, and G. H. Dalrymple. 1970. The early life history and ecology of *Ambystoma tigrinum* and *Ambystoma opacum* in New Jersey. American Midland Naturalist 84:474–495.

Hird, C., R. L. Cramp, and C. E. Franklin. 2023. Thermal compensation reduces DNA damage from UV radiation. Journal of Thermal Biology 117:103711.

Hornbach, D. J., E. G. Schilling, and H. Kundel. 2020. Ecosystem metabolism in small ponds: the effects of floating-leaved macrophytes. Water 12:1458.

Immonen, E. V., I. Ignatova, A. Gislen, E. Warrant, M. Vähäsöyrinki, M. Weckström, and R. Frolov. 2014. Large variation among photoreceptors as the basis of visual flexibility in the common backswimmer. Proceedings of the Royal Society B 281:20141177.

Isayama, T., Y. Chen, M. Kono, E. Fabre, M. Slavsky, W. J. DeGrip, J. X. Ma, R. K. Crouch, and C. L. Makino. 2014. Co-expression of three opsins in cone photoreceptors of the salamander *Ambystoma tigrinum*. Journal of Comparative Neurology 522:2249–2265.

Juhasz-Dora, T., T. Thesslund, J. Maguire, T. Doyle, and S. Lindberg. 2024. Investigation of biofluorescence produced by the red king crab *Paralithodes camtschaticus*. Aquaculture, Fish and Fisheries 4:159.

Kelley, J. L., I. Taylor, N. S. Hart, and J. C. Partridge. 2017. Aquatic prey use countershading camouflage to match the visual background. Behavioral Ecology 28:1314–1322.

Kerney, R., E. Kim, R. P. Hangarter, A. A. Heiss, C. D. Bishop, and B. K. Hall. 2011. Intracellular invasion of green algae in a salamander host. Proceedings of the National Academy of Sciences of the United States of America 108:6497–6502.

Kim, E., Y. Lin, R. Kerney, L. Blumenberg, and C. Bishop. 2014. Phylogenetic analysis of algal symbionts associated with four North American amphibian egg masses. PLoS ONE 9:e108915.

Kohler, A. M., E. R. Olson, J. G. Martin, and P. S. Anich. 2019. Ultraviolet fluorescence discovered in New World flying squirrels (*Glaucomys*). Journal of Mammalogy 100:21–30.

Kong, B., K. Preston, M. Ishimatsu, and E. Adelsheim. 2023. Biofluorescence in the California Tiger Salamander, *Ambystoma californiense* (Amphibia: Ambystomatidae). Herpetology Notes 16:161–163.

Krause-Jensen, D., and K. Sand-Jensen. 1998. Light attenuation and photosynthesis of aquatic plant communities. Limnology and Oceanography 43:396–407.

Lamb, J. Y., and M. P. Davis. 2020. Salamanders and other amphibians are aglow with biofluorescence. Scientific Reports 10:2821.

Lannoo, M. J. (Ed.). 2005. Amphibian Declines: The Conservation Status of United States Species. University of California Press, Berkeley, California.

Lean, D. 1998. Attenuation of solar radiation in humic waters, p. 109–124. *In*: Aquatic Humic Substances: Ecology and Biogeochemistry. D. O. Hessen and L. H. Tranvik (eds.). Springer-Verlag, Berlin, Heidelberg.

Liebman, P. A., and G. Entine. 1968. Visual pigments of frog and tadpole (*Rana pipiens*). Vision Research 8:761–775.

Liedtke, H. C., K. Lopez-Hervas, I. Galván, N. Polo-Cavia, and I. Gomez-Mestre. 2023. Background matching through fast and reversible melanin-based pigmentation plasticity in tadpoles comes with morphological and antioxidant changes. Scientific Reports 13:12064.

Maia, R., H. Gruson, J. A. Endler, and T. E. White. 2019. pavo 2: new tools for the spectral and spatial analysis of colour in R. Methods in Ecology and Evolution 10:1097–1107.

Marshall, J., and S. Johnsen. 2017. Fluorescence as a means of colour signal enhancement. Philosophical Transactions of the Royal Society B 372:20160335.

McGraw, K. J. 2006. Mechanisms of carotenoid-based coloration, p. 177–242. *In*: Bird Coloration, Vol I: Mechanisms and Measurements. G. E. Hill and K. J. McGraw (eds.). Harvard University Press, Cambridge, Massachusetts.

Montgomerie, R. 2006. Analyzing colors, p. 90–147. *In*: Bird Coloration, Vol I: Mechanisms and Measurements. G. E. Hill and K. J. McGraw (eds.). Harvard University Press, Cambridge, Massachusetts.

Petranka, J. W. 1998. Salamanders of the United States and Canada. Smithsonian Institution Press, Washington, D.C.

Petranka, J. W., A. W. Rushlow, and M. E. Hopey. 1998. Predation by tadpoles of *Rana sylvatica* on embryos of *Ambystoma maculatum*: implications of ecological role reversals by *Rana* (predator) and *Ambystoma* (prey). Herpetologica 54:1–13.

Polo-Cavia, N., and I. Gomez-Mestre. 2017. Pigmentation plasticity enhances crypsis in larval newts: associated metabolic cost and background choice behavior. Scientific Reports 7:39739.

Rodríguez-Rodríguez, E. J., J. F. Beltrán, and R. Márquez. 2021. Melanophore metachrosis response in amphibian tadpoles: effect of background colour, light and temperature. Amphibia-Reptilia 42:133–140.

Salthe, S. N. 1965. Increase in volume of the perivitelline chamber during development of *Rana pipiens* (Schreber). Physiological Zoology 38:80–98.

Shi, D., and J. Boucaut. 1995. The chronological development of the urodele amphibian *Pleurodeles waltl* (Michah). The International Journal of Developmental Biology 39:427–441.

Smith, W. L., C. A. Buck, G. S. Ornay, M. P. Davis, R. P. Martin, S. Z. Gibson, and M. G. Girard. 2018. Improving vertebrate skeleton images: fluorescence and the non-permanent mounting of cleared-and-stained specimens. Copeia 106:427–435.

Sparks, J. S., R. C. Schelly, W. L. Smith, M. P. Davis, D. Tchernov, V. A. Pieribone, and D. F. Gruber. 2014. The covert world of fish biofluorescence: a phylogenetically widespread and phenotypically variable phenomenon. PLoS ONE 9:e83259.

Spicer, M. M., A. N. Stokes, T. L. Chapman, E. D. Brodie Jr., E. D. Brodie III, and B. G. Gall. 2018. An investigation into tetrodotoxin (TTX) levels associated with the red dorsal spots in Eastern Newt (*Notophthalmus viridescens*) efts and adults. Journal of Toxicology 2018:9196865.

Stretz, P., T. L. Anderson, and J. J. Burkhart. 2019. Macroinvertebrate foraging on larval *Ambystoma maculatum* across ontogeny. Copeia 107:244–249.

Taboada, C., A. E. Brunetti, F. N. Pedron, F. Carnevale Neto, D. A. Estrin, S. E. Bari, L. B. Chemes, N. Peporine Lopes, M. G. Lagorio, and J. Faivovich. 2017. Naturally occurring fluorescence in frogs. Proceedings of the National Academy of Sciences of the United States of America 114:3672–3677.

Thibaudeau, G., and R. Altig. 2012. Coloration of anuran tadpoles (Amphibia): development, dynamics, function, and hypotheses. International Scholarly Research Notices 2012:725203.

Ward, D., and O. J. Sexton. 1981. Anti-predator role of salamander egg membranes. Copeia 1981:724–726.

Whitcher, C., L. Beaver, and E. Moriarty Lemmon. 2024a. The effect of biofluorescence on predation upon Cope's gray treefrog: a clay model experiment. Behavioral Processes 215:104996.

Whitcher, C., S. R. Ron, F. Ayala-Varela, A. J. Crawford, V. Herrera-Alva, E. F. Castillo-Urbina, F. Grazziotin, R. M. Bowman, A. R. Lemmon, and E. Moriarty Lemmon. 2024b. Evidence for ecological tuning of anuran biofluorescent signals. Nature Communications 15:8884.

Wilcox, A., and S. Lewis. 2019. Fluorescence in fireflies (Coleoptera: Lampyridae): using sentinel prey to investigate a possible aposematic signal. Florida Entomologist 102:614–618.

Yergeau, D. A., M. R. Johnson Hamlet, E. Kuliyev, H. Zhu, J. R. Doherty, T. D. Archer, A. P. Subhawong, M. B. Valentine, C. M. Kelley, and P. E. Mead. 2009. Transgenesis in *Xenopus* using the Sleeping Beauty transposon system. Developmental Dynamics 238:1727–1743.